

Switching of absorptive nonlinearity from reverse saturation to saturation in polymer-ZnO nanotop composite films

P. C. Haripadmam,¹ Honey John,² Reji Philip,³ and Pramod Gopinath^{1,a)}

¹Department of Physics, Indian Institute of Space Science and Technology, Thiruvananthapuram 695 547, India

²Department of Chemistry, Indian Institute of Space Science and Technology, Thiruvananthapuram 695 547, India

³Light and Matter Physics Group, Raman Research Institute, Sadashivanagar, Bangalore 560 080, India

(Received 18 September 2014; accepted 19 November 2014; published online 1 December 2014)

We report an interesting switchover of optical nonlinearity from Reverse Saturable Absorption (RSA) to Saturable Absorption (SA) in polymer-Zinc Oxide (ZnO) nanotop composite films, investigated using the Z-scan technique. The nanocomposites have been prepared by *in situ* polymerization of the monomer in which ZnO nanotops are dispersed with the help of a dispersing agent. The films exhibit RSA for lower concentrations of ZnO nanotops, which changes to SA on increasing the loading concentration, irrespective of the monomer and dispersing agent used. These versatile films are good candidates for applications such as ultrafast optical switching and optical limiting. © 2014 AIP Publishing LLC. [<http://dx.doi.org/10.1063/1.4903073>]

Interaction of intense light with materials can cause substantial changes to their optical absorption, resulting in intensity dependent transmittance known as nonlinear absorption (NLA). Investigation of nonlinear absorption is significant owing to its wide range of applications in photonics. Suitable materials which exhibit NLA are required for optoelectronic device fabrication.^{1–4} Nonlinear absorption can take the form of either saturable absorption (SA) or reverse saturable absorption (RSA) depending on the incident wavelength, fluence, pulse duration, and material concentration.^{5–7} Saturable absorbers exhibit an enhanced transmittance at higher incident light intensities, whereas reverse saturable absorbers exhibit a decrease in transmittance with intensity.⁸ In material systems, saturable absorption becomes prominent when the incident intensity is high enough so that the ground state population is depleted and the population of the upper and lower states tends to equalize. On the other hand, effects like two-photon absorption (TPA), multiphoton absorption, excited state absorption, and free carrier absorption, or a combination of these, can cause reverse saturable absorption.⁹ Saturable absorbers are widely utilized in Q-switching and mode-locking³ to produce short and ultrashort laser pulses.¹⁰ Reverse saturable absorbers can be used as optical power limiters and molecular spatial light modulators (SLM).¹

Depending primarily on the excitation wavelength, materials might behave either as saturable absorbers or as reverse saturable absorbers. A transition from RSA to SA or vice versa may be observed when experimental parameters are changed. Reports of such behaviour include intensity dependent switchover in organic dyes and metals,^{11–14} and concentration dependent switchover in organic dyes,⁶ dye-polymer films,¹⁵ and metal doped semiconductors.¹⁶ A limited number of SA/RSA switching studies have been performed in semiconductors,^{16–19} particularly in metal doped semiconductors^{17,18} and semiconductor-semiconductor compounds.¹⁹

Finding and investigating new materials exhibiting this transition behavior is of importance in view of its many applications. For instance, a combination of RSA and SA is good for mode-locking and pulse shaping, when placed between high power laser amplifiers in oscillator-amplifier chains.^{1,20} Similarly, an RSA-SA combination performs as an optical diode.^{21,22} They can also be utilized as optical pulse compressors in laser amplifier chains to eliminate the wings of short optical pulses.²³

ZnO is a versatile material having wide variety of applications including optical limiting.^{24–27} Here, we report the reversal of nonlinear absorption in polymer-ZnO nanotop composite films where the films switch from RSA to SA nature upon increasing the loading concentration of ZnO. The ZnO nanotops used in this study are neither doped with any impurity nor mixed with any semiconductor to alter its properties.

ZnO nanoparticles having an average crystallite size of 23 nm are synthesized from zinc acetate dihydrate (Merck). The nanoparticles have the shape of tops and are therefore called ZnO nanotops. Detailed synthesis, film fabrication, and property evaluation are reported elsewhere.²⁴ For better quality films, a dispersing agent (oleic acid) is used to disperse the ZnO nanotops. Oleic acid dispersed nanoparticles are then dispersed well in methyl methacrylate by ultrasonication. Composites of the ZnO nanotops with Poly methylmethacrylate (PMMA) are prepared by the *in situ* bulk polymerisation technique. The concentration of ZnO nanotops in the composite is varied from 1 wt. % to 10 wt. %, and the composites were fabricated on a glass substrate by spin coating. In all cases, the number of coatings is maintained at three. With respect to the loading concentration of ZnO in the matrix, the films are named from F10 through F100. Another set of films is prepared using the dispersing agent triton by the same procedure, and the films are named FIT through F10T.

The surface morphology of the PMMA-ZnO nanotop composite films is analyzed using Scanning electron microscopy (SEM) (FEI Quanta FEG 200 High Resolution Scanning Electron Microscope). Figures 1(a) and 1(c) show the SEM

^{a)}Author to whom correspondence should be addressed. Electronic mail: pramod@iist.ac.in

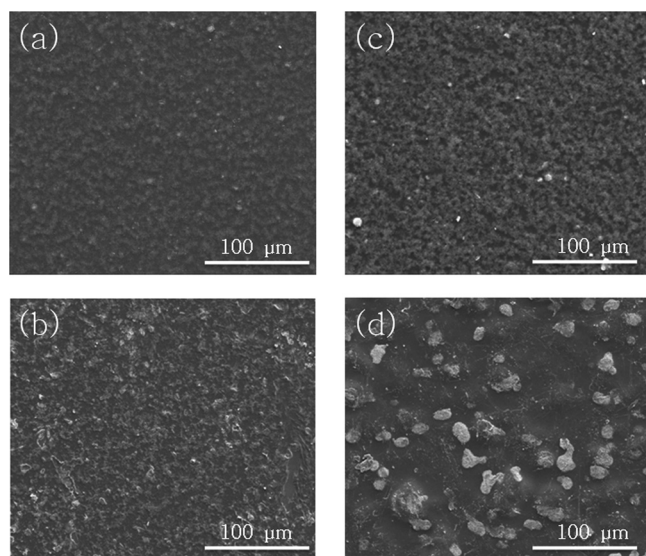


FIG. 1. SEM images of (a) F2O, (b) F2T, (c) F8O, and (d) F8T.

images of the films prepared in the presence of oleic acid for lower (2 wt. %) and higher (8 wt. %) concentrations of ZnO nanotops. Figures 1(b) and 1(d) show SEM images of the films prepared in the presence of triton. It is very clear from the images that the presence of oleic acid improves the dispersion of nanoparticles in the polymer matrix.

Room temperature absorption spectra (Cary 100 Bio UV-Visible spectrophotometer) of the films measured for 2 wt. % (F2) and 8 wt. % (F8) loading concentrations of ZnO are shown in Figure 2(a). Plots 1 and 3 correspond to films prepared in the presence of triton, whereas plots 2 and 4 correspond to films prepared in the presence of oleic acid. It is clear from the spectra that UV absorption increases with increase in loading concentration of ZnO nanotops in the matrix. Optical bandgap of the films is calculated using Tauc plots as shown in Figure 2(b).

Figure 3 shows the photoluminescence spectra of films with 8 wt. % nanoparticles in the monomer. A clear band edge emission is observable from Figure 3, due to the photo-generated electron recombination with holes in the valence band or in traps near the valence band.²⁸ The films also emit in the red-NIR region, which can be attributed to the presence of excess oxygen.²⁹ Band edge emission is more intense compared to red-NIR emission, and the films prepared using triton emit more compared to those prepared using oleic acid.

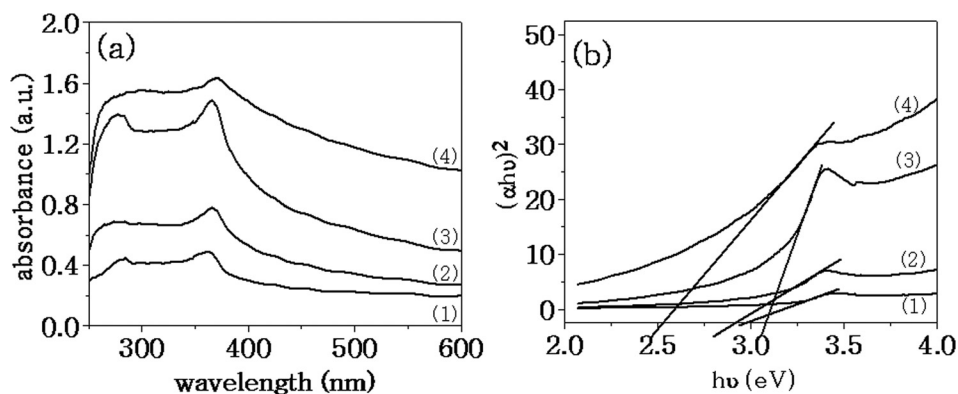


FIG. 2. (a) UV-visible absorption spectra, and (b) Tauc plots of the films. (1) F2T, (2) F2O, (3) F8T, and (4) F8O.

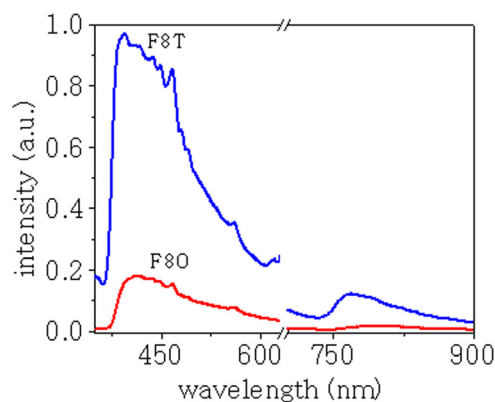


FIG. 3. Photoluminescence spectra of 8 wt. % ZnO films with oleic acid and triton as dispersing agents. Excitation is at 325 nm.

Open aperture Z-scan³⁰ measurements of the films are carried out using a Q-switched Nd:YAG laser (7 ns and 532 nm). The laser is run in the single-shot mode in order to avoid sample heating and thermal nonlinearities. The sample is mounted on a computer controlled linear translation stage, which is moved along the Z-axis through the focal point of a lens, of focal length 10.5 cm. The beam waist ω_0 is calculated to be 26 μm and the Rayleigh length, Z_0 , evaluated using the equation⁸

$$Z_0 = \frac{\pi\omega_0^2}{\lambda} \quad (1)$$

is found to be 3.99 mm. This is larger than the sample thickness, which is an essential requirement for the validity of the Z-scan theory suggested by Bahae *et al.*³⁰ The transmitted beam energy and the reference beam energy are measured simultaneously by an energy ratio meter (Rj7600, Laser Probe Corp.) using two identical pyroelectric detector heads (Rjp735).

The data obtained from the experiment are found to fit well to a third order nonlinear absorption process, according to the nonlinear transmission equation

$$T(z, S = 1) = \left(\frac{1}{\sqrt{\pi}q_0(z, 0)} \right) \int_{-\infty}^{\infty} \ln \left[1 + q_0(z, 0)e^{-\tau^2} \right] d\tau, \quad (2)$$

where $q_0(z, 0) = \beta I_0 L_{\text{eff}}$, with β being the NLA coefficient. I_0 is the incident irradiance at the beam focus ($z = 0$). The effective sample thickness, L_{eff} , is given by

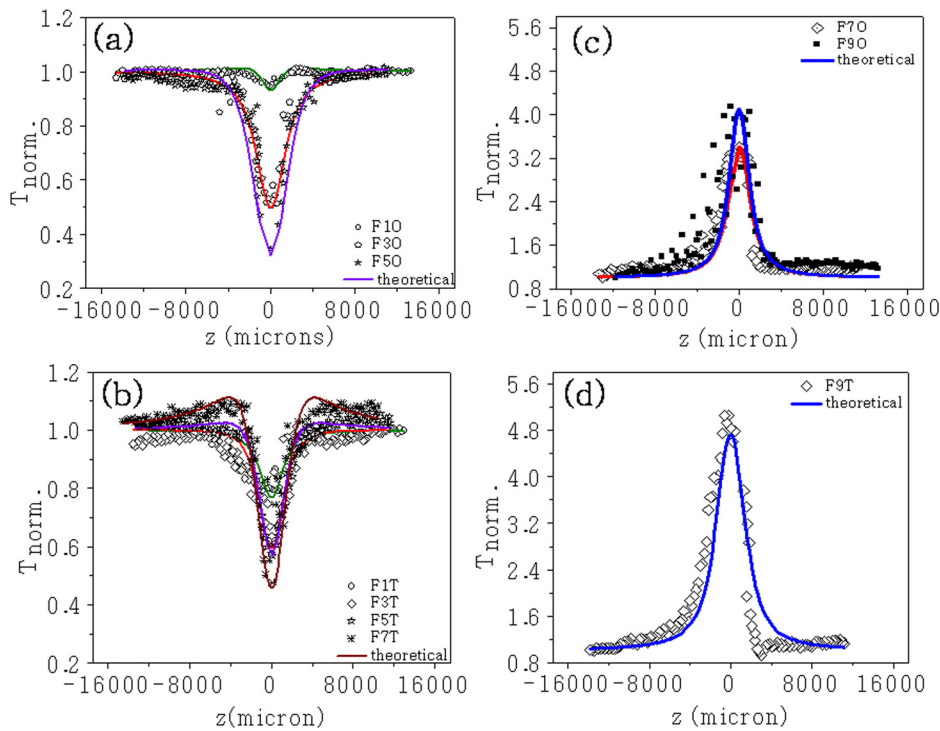


FIG. 4. Open aperture Z-scan curves of the films showing RSA [(a) and (b)] and SA [(c) and (d)].

$$L_{eff} = \frac{(1 - e^{-\alpha L})}{\alpha}, \quad (3)$$

where L is the film thickness and α is the linear absorption coefficient.

Figure 4 shows the optical limiting response of all the films for an input laser pulse energy $30 \mu\text{J}$, with ZnO loading concentration varying from 1 wt. % to 9 wt. %. Figures 4(a) and 4(c) correspond to the films prepared in the presence of oleic acid, whereas Figures 4(b) and 4(d) correspond to the films prepared in the presence of triton. In both cases, the film with maximum loading concentration (10 wt. %) is found to be getting damaged by the laser.

The third order NLA coefficient and saturation intensity calculated for all the films are given in Table I. For the films prepared using oleic acid, up to 5 wt. % loading of ZnO in the matrix, the RSA property gets progressively enhanced. However, for films with higher ZnO loading (from 6 wt. % to 9 wt. %), the nonlinearity switches over to SA. In the case of films prepared in the presence of triton, the RSA-SA transition appeared only above 7 wt. % of ZnO loading. On the

other hand, undoped films (made with PMMA and dispersing agent only) did not show any nonlinearity, indicating that the observed nonlinearity arises exclusively from the ZnO nanotops.

Figure 5 shows the optical limiting response of the films, prepared with ZnO nanotops dispersed in triton and a mixture of polystyrene (PS) and PMMA (1:1). Two composites with 6 wt. % (PF6T) and 8 wt. % (PF8T) of the nanoparticles in the monomer are chosen for the fabrication of films. Figure 5 clearly depicts that PF6T exhibits RSA, whereas PF8T exhibits SA. The effective nonlinear absorption coefficient is calculated to be 7900 cm/GW for PF6T and 1400 cm/GW for PF8T.

Figures 4 and 5 clearly show that the composite films exhibit RSA at lower concentrations and SA at higher concentrations, regardless of the polymer matrix or the dispersing agent used. During the preparation and fabrication of polymer-ZnO nanotop composite films, the ZnO nanotops get trapped inside the polymer chains. Thus in addition to the dispersing agent, the matrix also helps to get a well dispersed nanocomposite. As a result, the nanoparticles in the

TABLE I. Parameters calculated for the films.

| Film | Dispersing agent | β_{eff} (cm/GW) | I_{sat} (GW/cm ²) | Film | Dispersing agent | β_{eff} (cm/GW) | I_{sat} (GW/cm ²) |
|------|------------------|-----------------------|---------------------------------|------|------------------|-----------------------|---------------------------------|
| F10 | Oleic acid | 260 | 1.00 | F1T | Triton | 270 | 0.98 |
| F20 | | 620 | 0.95 | F2T | | 560 | 0.95 |
| F30 | | 2400 | 0.95 | F3T | | 1500 | 0.65 |
| F40 | | 6400 | 0.22 | F4T | | 2600 | 0.52 |
| F50 | | 12000 | 0.22 | F5T | | 3200 | 0.50 |
| F60 | | 1700 | 0.62 | F6T | | 6600 | 0.32 |
| F70 | | 310 | 0.62 | F7T | | 7000 | 0.24 |
| F80 | | 260 | 0.62 | F8T | | 80 | 0.25 |
| F90 | | 180 | 0.62 | F9T | | 10 | 0.26 |

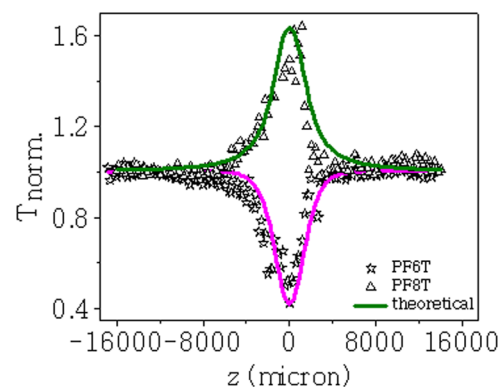


FIG. 5. Open aperture Z-scan curves measured for PS/PMMA-ZnO nanotop composite films.

film are not much hindered from exhibiting their inherent properties. When these films are exposed to laser pulses, electric charge interaction between the polymer and the nanoparticle can create a dielectric dipole layer on the nanoparticle surface, which is known as the dielectric confinement effect. This is a surface polarization effect depending on the permittivity ratio of the particles and the surrounding medium.³¹ It can accelerate the separation of excited charges so as to enhance the electric field inside the nanoparticles.^{32,33} At the same time, it can change the charge density distribution of the nanoparticle surface, strengthening anharmonic vibrations of surface electrons.³⁴ Thus, the nanocomposites will be able to exhibit stronger nonlinear response.

In our case, the Z-scan data fit well to a theoretical model where both saturable absorption and two-photon absorption take place in the system, as shown in Figures 4 and 5. From the bandgap (E_g) values of the selected films obtained from the Tauc plot (Figure 2(b)), it can be confirmed that the excitation photon energy ($h\nu = 2.33$ eV) fulfills the requirement for TPA, which is $h\nu < E_g < 2h\nu$.³⁵

From the linear absorption spectra of the films (Fig. 2(a)), it is obvious that the films have some absorption at the excitation wavelength (532 nm). The films have more absorption at the two-photon wavelength of 266 nm, indicating the existence of excited states suitable for two-step as well as genuine two-photon absorption processes.^{36,37} As the measured NLA coefficients are found to vary with incident intensity in our samples, the observed NLA should have less contribution from genuine TPA and more contribution from a two-step absorption process.^{38–41} Since the laser pulse-width used for the present study (7 ns) is greater than the free carrier lifetime of ZnO nanoparticles,⁴² there is a chance for strong free carrier absorption (FCA) by the photogenerated carriers. The variation of NLA coefficient with intensity also confirms this fact.⁴³ Thus, in general, TPA, two-step absorption, and FCA have distinct roles in the observed nonlinear absorption of our samples.

The Z-scan plots (Figures 4(c), 4(d), and 5) show that films with higher ZnO concentration exhibit saturable absorption. SA is related to the process of electron excitation from the valence band to the conduction band by photon absorption. Once the electrons accumulate in the conduction band and some of them undergo FCA, the initial states of the absorbing transition will be depleted and the final states will get occupied. As a result, further absorption is reduced. This effect is known as Pauli blocking.⁴⁴ Pauli blocking is a consequence of the exclusion principle according to which electron transitions are inhibited if the final state is occupied by another electron. According to Zitter,⁴⁵ who has given a theoretical framework for this phenomenon, a semiconductor absorbing a monochromatic light beam will generate enough number of carriers to fill band states up to and including those of the optical transition. Optical absorption will be then saturated and a condition of transparency shall result. The study shows that in this regime, the absorption coefficient varies inversely with light intensity.

The nonlinear absorption coefficients corresponding to the maximum loading concentrations in the RSA regime are found to be 12 000 cm/GW, 7000 cm/GW, and 7900 cm/GW, for F5O, F7T, and PF6T, respectively. Thus, it is clear that

oleic acid dispersed film has higher nonlinearity compared to triton dispersed film. This is because of the efficiency of oleic acid to provide a well dispersed medium for laser absorption, as observed from Figure 1. Films prepared in the presence of dispersing agents have exhibited an enhanced NLA coefficient compared to films prepared without dispersing agent, which has been reported earlier.²⁴

To conclude, polymer-ZnO nanotop composite films are fabricated for different loading concentrations of ZnO. The films exhibit good UV absorption properties. A concentration dependent transition from reverse saturable absorption to saturable absorption is observed when the films are irradiated by nanosecond laser pulses at 532 nm. These films are potential candidates for technological applications, such as optical limiting, Q-switching, and mode-locking, and for designing novel photonic devices.

Authors thank SAIF, IIT Madras, for SEM measurements.

¹K. P. J. Reddy, *Curr. Sci.* **61**, 520 (1991), available at http://www.currentscience.ac.in/Downloads/article_id_061_08_0520_0526_0.pdf.

²Y. B. Band and B. Scharf, *Chem. Phys. Lett.* **127**, 381 (1986).

³Y. X. Fan, J. L. He, Y. G. Wang, S. Liu, H. T. Wang, and X. Y. Ma, *Appl. Phys. Lett.* **86**, 101103 (2005).

⁴S. M. Kobtsev, S. V. Kukarin, and Y. S. Fedotov, *Laser Phys.* **21**, 283 (2011).

⁵J. Wang and W. J. Blau, *J. Opt. A: Pure Appl. Opt.* **11**, 024001 (2009).

⁶R. Philip, G. R. Kumar, N. Sandhyarani, and T. Pradeep, *Phys. Rev. B* **62**, 13160 (2000).

⁷R. S. S. Kumar, S. V. Rao, L. Giribabu, and D. N. Rao, *Chem. Phys. Lett.* **447**, 274 (2007).

⁸R. L. Sutherland, *Handbook of Nonlinear Optics* (Marcel Dekker, New York, 2003).

⁹L. Irirpan, A. Deepthy, B. Krishnan, V. P. N. Nampoori, and P. Radhakrishnan, *Appl. Phys. B* **90**, 547 (2008).

¹⁰T. R. Schibli, K. Minoshima, H. Kataura, E. Itoga, N. Minami, S. Kazaoui, K. Miyashita, M. Tokumoto, and Y. Sakakibara, *Opt. Express* **13**, 8025 (2005).

¹¹J. W. Perry, K. Mansour, S. R. Marder, K. J. Perry, D. Alvarez, and I. Choong, *Opt. Lett.* **19**, 625 (1994).

¹²U. Gurudas, E. Brooks, D. M. Bubb, S. Heiroth, T. Lippert, and A. Wokaun, *J. Appl. Phys.* **104**, 073107 (2008).

¹³Y. Gao, X. Zhang, Y. Li, H. Liu, Y. Wang, Q. Chang, W. Jiao, and Y. Song, *Opt. Commun.* **251**, 429 (2005).

¹⁴R. Philip, P. Chantharasupawong, H. Quian, R. Jin, and J. Thomas, *Nano Lett.* **12**, 4661 (2012).

¹⁵G. Sreekumar, P. G. L. Frobel, C. I. Muneera, K. Sathiyamoorthy, C. Vijayan, and C. Mukherjee, *J. Opt. A: Pure Appl. Opt.* **11**, 125204 (2009).

¹⁶R. A. Ganeev, A. I. Rysanysky, A. L. Stepanov, and T. Usmanov, *Phys. Status Solidi B* **241**, R1 (2004).

¹⁷L. Li and S. X. Rui, *Chin. Phys. B* **17**, 2170 (2008).

¹⁸K. Zhang, J. Li, W. Wang, J. Xiao, W. Yin, and L. Yu, *Opt. Lett.* **36**, 3443 (2011).

¹⁹L. Irirpan, V. P. N. Nampoori, and P. Radhakrishnan, *J. Appl. Phys.* **103**, 094914 (2008).

²⁰D. J. Harter, Y. B. Band, and E. P. Ippen, *IEEE J. Quantum Electron.* **21**, 1219 (1985).

²¹B. Anand, R. Podila, K. Lingam, S. R. Krishnan, S. S. S. Sai, R. Philip, and A. M. Rao, *Nano Lett.* **13**, 5771 (2013).

²²R. Philip, M. Anija, C. S. Yelleswarapu, and D. V. G. L. N. Rao, *Appl. Phys. Lett.* **91**, 141118 (2007).

²³Y. B. Band, D. J. Harter, and R. Bavli, *Chem. Phys. Lett.* **126**, 280 (1986).

²⁴P. C. Haripadmam, M. K. Kavitha, H. John, B. Krishnan, and P. Gopinath, *Appl. Phys. Lett.* **101**, 071103 (2012).

²⁵H. Kind, H. Yan, B. Messer, M. Law, and P. Yang, *Adv. Mater.* **14**, 158 (2002).

²⁶M. M. A. El-Hady, A. Farouk, and S. Sharaf, *Carbohydr. Polym.* **92**, 400 (2013).

²⁷Y. S. Choi, J. W. Kang, D. K. Hwang, and S. J. Park, *IEEE Trans. Electron Devices* **57**, 26 (2010).

- ²⁸H. M. Xiong, *J. Mater. Chem.* **20**, 4251 (2010).
- ²⁹A. B. Djurišić and Y. H. Leung, *Small* **2**, 944 (2006).
- ³⁰M. S. Bahae, A. A. Said, T. H. Wei, D. J. Hagan, and E. W. van Stryland, *IEEE J. Quantum Electron.* **26**, 760 (1990).
- ³¹T. Takagahara, *Phys. Rev. B* **47**, 4569 (1993).
- ³²X. Wu, R. Wang, B. Zou, P. Wu, L. Wang, J. Xu, and W. Huang, *Appl. Phys. Lett.* **71**, 2097 (1997).
- ³³X. Ai, H. Fei, Y. Yang, L. Han, R. Nie, Y. Zhang, C. Zhao, L. Xiao, T. Li, J. Zhao, and J. Yu, *J. Lumin.* **60**, 364 (1994).
- ³⁴S. X. Wang, L. D. Zhang, H. Su, Z. P. Zhang, G. H. Li, G. W. Meng, and J. Zhang, *Phys. Lett. A* **281**, 59 (2001).
- ³⁵K. V. Adarsh, K. S. Sangunni, C. S. S. Sandeep, R. Philip, S. Kokenyesi, and V. Takats, *J. Appl. Phys.* **102**, 026102 (2007).
- ³⁶A. P. R. Mary, C. S. S. Sandeep, T. N. Narayanan, R. Philip, P. Moloney, P. M. Ajayan, and M. R. Anantharaman, *Nanotechnology* **22**, 375702 (2011).
- ³⁷J. Khatei, C. S. S. Sandeep, R. Philip, and K. S. R. K. Rao, *Appl. Phys. Lett.* **100**, 081901 (2012).
- ³⁸G. S. He, L.-S. Tan, Q. Zheng, and P. N. Prasad, *Chem. Rev.* **108**, 1245 (2008).
- ³⁹V. S. Muthukumar, R. Podila, B. Anand, S. S. S. Sai, K. Venkataramaniah, R. Philip, and A. M. Rao, *Encyclopedia of Nanotechnology* (Springer, Heidelberg, 2013).
- ⁴⁰S. Couris, E. Koudoumas, A. A. Ruth, and S. Leach, *J. Phys. B: At., Mol. Opt. Phys.* **28**, 4537 (1995).
- ⁴¹M. Rumi and J. W. Perry, *Adv. Opt. Photonics* **2**, 451 (2010).
- ⁴²X. J. Zhang, W. Ji, and S. H. Tang, *J. Opt. Soc. Am. B* **14**, 1951 (1997).
- ⁴³P. A. Kurian, C. Vijayan, C. S. S. Sandeep, R. Philip, and K. Sathiyamoorthy, *Nanotechnology* **18**, 075708 (2007).
- ⁴⁴Q. Bao, H. Zhang, Y. Wang, Z. Ni, Y. Yan, Z. X. Shen, K. P. Loh, and D. Y. Tang, *Adv. Funct. Mater.* **19**, 3077 (2009).
- ⁴⁵R. N. Zitter, *Appl. Phys. Lett.* **14**, 73 (1969).